RSC Advances

PAPER

View Article Online
View Journal | View Issue

Cite this: *RSC Adv.*, 2018, **8**, 1737

Highly efficient mesoporous polymer supported phosphine-gold(I) complex catalysts for amination of allylic alcohols and intramolecular cyclization reactions†

Huoliang Gu,‡ Xiong Sun,‡ Yong Wang, Haihong Wu * and Peng Wu *

Received 16th November 2017
Accepted 18th December 2017

DOI: 10.1039/c7ra12498h

rsc.li/rsc-advances

A series of novel heterogeneous gold(I) catalysts were synthesized by immobilizing gold(I) complexes on ordered mesoporous polymer FDU-15 and characterized by XRD, N_2 adsorption–desorption, FT-IR, TEM, EDS, *etc.* The catalytic activities of these catalysts were evaluated by the amination reactions of allylic alcohols. Among the catalysts investigated, FDU-(*p*-CF_3Ph)$_2$PAuCl (**3d**) was identified as the most efficient catalyst. Compared to the homogeneous catalyst, the enhanced catalytic activity of the heterogeneous gold(I) catalyst is closely related to the mesoporous structure of FDU-15. The catalytic system was suitable for a broad range of substrates and can be easily recovered and recycled at least twelve times without significant loss of catalytic activity. In addition, the catalytic performance of **3d** was further examined for intramolecular cyclization for the synthesis of heterocyclic compounds.

1. Introduction

The great potential of homogeneous gold(I) complex catalysts for chemical transformations has attracted increasing interest in numerous fields of research.[1–6] In this context, numerous homogeneous gold(I) complex-catalyzed reactions have been explored for the construction of carbon–carbon or carbon–heteroatom bonds, which are prevalent in many important pharmaceutical and bioactive natural products.[7–13] However, homogeneous catalysts often suffer from several drawbacks related to the handling of sensitive metal–ligand complexes, deactivation during reaction and difficulty in recovery and reuse of expensive reagents, which hinders their practical applications in industrial processes. One of the most promising approaches to overcome these drawbacks is to generate heterogeneous gold(I) catalysts.[14–20]

The use of heterogeneous catalysts has multiple advantages in both industrial and environmental concerns. Various types of materials, such as mesoporous silica and amorphous polymer, have been employed to support the gold(I) catalysts. Corma *et al.*[21] have immobilized a gold–carbene complex on mesostructured silicates and applied them for the hydrogenation of alkenes and the Suzuki reaction. Yu *et al.*[22] have described a polystyrene-immobilized gold(I) complex, which shows remarkable catalytic activities in three model transformations. Toste *et al.*[23] have developed silica-supported cationic gold(I) complexes, which exhibit superior reactivity in intramolecular additions of allenes with alkynes. Cai *et al.*[24] have developed an efficient and easily recoverable magnetic nanoparticle supported gold(I) catalyst for the direct reductive amination reaction, which proceeded at room temperature. Very recently, Shi *et al.*[25] reported a PS-TA-Au(I) catalyst with good activity and chemoselectivity. Asensio *et al.*[26] developed silica-immobilized NHC-gold(I) complexes, which are efficient in hydration and cyclization. In our previous study, we have successfully immobilized a chiral gold catalyst and applied it for the asymmetric cycloaddition of 2-alkynyl-2-alken-1-ones with nitrones.[27] Despite these significant advances, the design and development of a new heterogeneous gold(I) catalyst system is still challenging.

The nature of support plays an important role in governing the catalytic activities of supported gold(I) species on it. The mesoporous material has a suitable pore size for easy functionalization, particularly with large molecules, such as phosphine linkers and long-chain alkyl alkoxysiloxanes. Moreover, the ordered mesopores with a larger specific surface area can enable uniform distribution of anchored functional groups and benefit to mass transfer. The discovery of a class of mesoporous resol resin, which is purely an organic framework, opens up new opportunities for the synthesis of novel heterogeneous gold(I) catalysts. In comparison to conventional silica-based MCM-41, SBA-15 and organic–inorganic hybrid mesoporous materials, this ordered mesopolymer shares the advantages of both

Shanghai Key Laboratory of Green Chemistry and Chemical Processes, School of Chemistry and Molecular Engineering, East China Normal University, North Zhongshan Rd. 3663, Shanghai, 200062, China. E-mail: hhwu@chem.ecnu.edu.cn; pwu@chem.ecnu.edu.cn; Fax: +86-21-6223-8510

† Electronic supplementary information (ESI) available. See DOI: 10.1039/c7ra12498h

‡ These authors contributed equally to this work.

mesostructures and conventional organic polymers.[28,29] Its uniform mesopores with strong hydrophobicity allow for the easy access of organic reactants to the active sites within the channels. Based on this concept, we have succeeded in creating several heterogeneous catalysts, which show good catalytic activities in some chemical transformations.[30–35] Herein, we further explored the performance of FDU-type mesopolymer as the support for homogeneous gold(I) catalysts. We synthesized a series of new supported gold(I) catalysts and studied their catalytic activities in amination of allylic alcohols[36] and intramolecular cyclization.[37,38] These reactions were chosen because of their high atomic-efficiency and the heterocyclic products are structural fragments, which are widely found in many pharmaceutical active compounds.

2. Experimental

2.1 General

All reactions were carried out under an atmosphere of Ar in flame-dried glassware with magnetic stirring. ^{1}H NMR spectra and ^{13}C NMR spectra were recorded on a Bruker 500 MHz spectrometer in DMSO-d_6 or $CDCl_3$. All signals are reported in ppm with the internal TMS signal at 0 ppm as a standard. Data for ^{1}H NMR spectra are reported as follows: chemical shift (ppm, referenced to TMS; s = singlet, d = doublet, t = triplet, dd = doublet of doublets, m = multiplet), coupling constant (Hz), and integration. Data for ^{13}C NMR are reported in terms of chemical shift (ppm) relative to residual solvent peak ($CDCl_3$: 77.0 ppm). Reactions were monitored by thin layer chromatography (TLC) using silica gel plates. Flash column chromatography was performed over silica gel (200–300 mesh). Dichloromethane and toluene were freshly distilled from CaH_2; THF and dioxane were freshly distilled from sodium metal prior to use. The X-ray diffraction (XRD) patterns were collected on a Bruker D8 ADVANCE instrument using Cu-Kα radiation (λ = 1.5418 Å) at 35 kV and 30 mA. Nitrogen adsorption–desorption isotherms were measured on a Quantachrome Autosorb-3B instrument after evacuating the samples at 423 K for 6 h. The specific surface areas were evaluated using the Brunauer–Emmett–Teller (BET) method and the pore distribution was calculated by the BJH method from adsorption branches of isotherms. The TEM images were recorded using a JEOL-JEM-2010 microscope after the specimens were dispersed in ethanol and placed on holed-copper grids. The Au loading was determined by inductively coupled plasma-atomic emission spectroscopy (ICP-AES).

2.2 Preparation of FDU-type mesopolymer and FDU-CH_2Cl

The FDU-type mesopolymer was prepared according to previously reported procedures.[28] Then, FDU-type material was chloromethylated with chloromethyl methyl ether to obtain FDU-CH_2Cl using $AlCl_3$ as a catalyst.[34]

2.3 Typical methods for preparation of catalysts 3a–3c

Ar_2PCl (7 mmol) was mixed with Li metal (14 mmol) in anhydrous THF (20 mL) under argon atmosphere at −5 °C; the mixture was stirred at r.t. for 8 h. The resultant solution was mixed with FDU-CH_2Cl (1 g) and stirred overnight at r.t. to obtain FDU-PPh_2. Following this, FDU-PPh_2 (1.5 g) was mixed with Me_2SAuCl (0.14 mmol) in THF (10 mL) under argon atmosphere, and stirred at r.t. overnight to obtain the catalysts, which were denoted as FDU-Ph_2PAuCl, FDU-(*o*-OMePh)$_2$PAuCl and FDU-(*p*-OMePh)$_2$PAuCl (**3a–3c**). The Au loadings were determined by inductively coupled plasma atomic emission spectroscopy (ICP-AES).

2.4 The preparation of catalyst 3d

(*p*-CF_3Ph)$_2$PCl (7 mmol) was mixed with metal Li (14 mmol) in anhydrous THF (20 mL) under argon atmosphere at −5 °C; the mixture was stirred at r.t. for 1 h. The resultant solution was mixed with FDU-CH_2Cl (1 g) and stirred 10 h at 40 °C to obtain a ligand-functionalized material, FDU-(*p*-CF_3Ph)$_2$P. Following this, FDU-(*p*-CF_3Ph)$_2$P (0.5 g) was mixed with Me_2SAuCl (0.15 g) in anhydrous THF (15 mL) under argon atmosphere, and stirred at r.t. overnight to obtain the catalyst, which was denoted as FDU-(*p*-CF_3Ph)$_2$PAuCl (**3d**).

2.5 General procedure for amination of allylic alcohols and reused of the catalyst

Under argon atmosphere, a mixture of catalyst **3d** (6.9 mg, 0.05 mol%) and AgOTf (0.13 mg, 0.05 mol%) in dry solvent (1 mL) was magnetically stirred for 10 min at room temperature. A solution of allylic alcohols **4** (1 mmol) and amine **5** (2 mmol) in dry solvent (1 mL) was added into the aforementioned suspension and stirred under argon atmosphere. The reaction was monitored by TLC. When the reaction was over, the catalyst was recovered by simple filtration. The filtrate was diluted with water and brine; the product was extracted with ethyl acetate (3 × 10 mL). The combined organic phase was dried over anhydrous $MgSO_4$ and concentrated under vacuum. The residue was purified by column chromatography on silica gel affording the product **6**. The catalyst was washed with ethyl acetate and water and then suspended in acetone for 30 min under ultrasonication. Then, the catalyst was filtered, dried at 50 °C under vacuum overnight and reused for the next cycle.

2.6 General procedure for the preparation of 2,3-dihydro-4*H*-pyran-4-ones

Under an argon atmosphere, AgOTf (5.8 mg, 5 mol%) was added into a suspension of **3d** (316.5 mg, 5 mol%) in 4 mL toluene at room temperature. The mixture was stirred for 10 min to generate the cationic gold catalyst. After the substrate **7** (0.45 mmol) was added, the reaction mixture was stirred at room temperature. The reaction was monitored by TLC. When the reaction was over, the catalyst was recovered by simple filtration. The filtrate was diluted with brine, and the product was extracted with ethyl acetate. The combined organic phase was dried over anhydrous $MgSO_4$ and concentrated under vacuum. The residue was purified by column chromatography on silica gel affording the product **8a–k**.

2.7 Synthesis of substituted furan catalyzed by 3d

AgOTf (0.1 mol%) was added to a solution of **3d** (0.1 mol%) in dry toluene at room temperature under an argon atmosphere. The mixture was stirred for 10 min to generate the gold(I) catalyst. After the substrate **9** was added, the reaction mixture was further stirred at room temperature. The reaction was monitored by TLC. When the reaction was completed, the catalyst was recovered by simple filtration. The filtrate was diluted with water and brine, and the product was extracted with ethyl acetate. The combined organic phase was dried over anhydrous $MgSO_4$ and concentrated under vacuum. The residue was purified by column chromatography on silica gel to afford the product **10**.

3. Results and discussion

3.1 Synthesis and characterization of catalysts

The strategy for the synthesis of FDU-type mesopolymer supported gold(I) catalysts **3a–3d** are shown in Scheme 1. The chloromethylated materials, FDU-CH_2Cl (**1**), were first prepared by anchoring the $-CH_2Cl$ groups to the benzene rings of the mesopolymers using $AlCl_3$ and then functionalizing with phosphine ligands to afford ligand-modified materials **2a–2d**. When **2a–2d** were subsequently stirred in anhydrous THF solution containing gold precursor under argon atmosphere, the gold(I) ions were coordinated to phosphine ligands to afford the catalysts **3a–3d**.

The powder X-ray diffraction (XRD) patterns of FDU-15 mesopolymer and the modified mesoporous materials are shown in Fig. 1 and S1 (ESI†). Although the diffraction peaks gradually decreased in intensity after stepwise modifications, all samples still showed well defined (10), (11), (20) planes of a 2D hexagonal structure (*P6mm*) for the FDU-15 mesopolymer, which proved that the mesostructures were well preserved in the entire process of catalyst preparation.

Fig. 2 and S2† show the N_2 adsorption–desorption isotherms and the corresponding pore size distributions of the parent and grafted FDU-15 samples. All samples displayed a typical type IV isotherm with apparent H2 hysteresis loops, implying that the samples possessed a mesoporous structure. The specific surface area (S_{BET}), pore diameter (D_p) and pore volume (V_p) were calculated using the BJH method from the desorption branches of the N_2 isotherm (Table 1). After post-modification, a gradual decrease in the BET surface areas, pore volume and average pore diameter was noted, presumably attributed to the incorporation of the organic groups (phosphine ligand) into the channels of FDU-type mesopolymer.

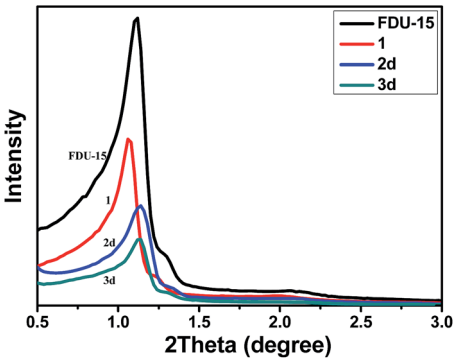

Fig. 1 Powder XRD patterns of (a) FDU-15, (b) **1**, (c) **2d** and (d) **3d**.

Transmission electron microscopy (TEM) images (Fig. 3) displayed highly ordered mesoporous arrays and long-range mesoporous channels for the parent and functionalized mesopolymers. The mesopore array of **3d** was a typical 2D hexagonal mesostructure, which verified that well-ordered mesoporous structures were maintained precisely after the gradual chemical grafting.

The samples before and after grafting were further characterized by FT-IR (Fig. S3†). The band at 3437 cm^{-1} is assigned to the phenolic hydroxyl stretching vibration. Comparing **1** with the parent FDU-type material, a new band appeared at 698 cm^{-1} after chloromethylation treatment, which is attributed to the stretching vibration of the C–Cl bond.[35] For sample **2d**, the new bands developed at 1065 cm^{-1} and 1167 cm^{-1} are assigned to the C–F bond stretching vibration. The band at 1323 cm^{-1} is assigned to the characteristic P-C vibration. These results demonstrated that the phosphine ligands were successfully introduced in the mesoporous polymers. No visible change was observed in IR spectra after further modification with Me_2SAuCl.

In addition, the samples before and after functionalization were characterized by EDS spectroscopy (Fig. S4†) and solid

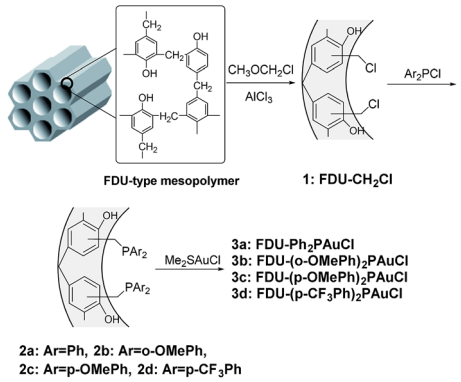

Scheme 1 The strategy for the synthesis FDU-type mesopolymer supported gold(I) catalysts **3a–3d**.

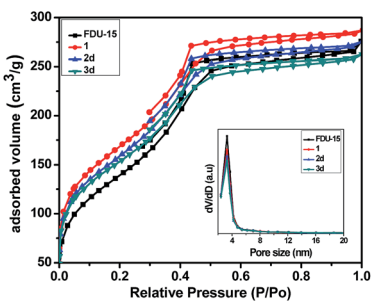

Fig. 2 The nitrogen adsorption–desorption isotherms and BJH pore size distribution curves of FDU-15, **1**, **2d** and **3d**.

Table 1 Textural properties of parent FDU-15 and grafted samples[a]

Sample	S_{BET} (m^2 g^{-1})	V_p (cm^3 g^{-1})	D_p[b] (nm)	Au[c] (wt%)
FDU-15	466	0.47	3.3	—
1	443	0.43	3.3	—
2a	421	0.41	3.2	—
2b	405	0.40	3.3	—
2c	417	0.40	3.3	—
2d	432	0.30	3.3	—
3a	417	0.40	3.2	2.6
3b	383	0.30	3.3	0.98
3c	397	0.40	3.3	1.0
3d	400	0.30	3.3	1.4

[a] Given by N_2 sorption at 77 K. [b] By BJH analysis. [c] ICP analysis.

state ^{13}C NMR spectroscopy (Fig. S5†). The characteristic peak of elemental Cl was observed after chloromethylation (Fig. S4b†). After the functionalization with chemical ligand and homogeneous gold catalyst, new characteristic peaks of elemental F and Au were noticed (Fig. S4c–d†). According to the ^{13}C NMR spectra, all samples show distinct signals at 35, 129 and 151 ppm, which are assigned to the methylene bridges, phenolic hydroxyl substitutions and other carbons in the phenol ring, respectively. Compared to FDU-15, the ligand-functionalized sample displayed a new band at 65 ppm, which corresponds to the methylene bridges between the phenol rings and ligands. The signals of the carbons in $-CF_3$ groups are not visible, which may overlap with the other carbon in the phenol ring. These spectra further confirmed the successful functionalization of FDU-CH_2Cl with the ligand and the homogeneous gold catalyst. Moreover, the binding energy at 85.1 eV of Au XPS spectrum (Fig. S6†) for fresh catalyst-**3d** clearly confirms the presence of Au(I) species. The Au loadings were determined to be 2.6, 0.98, 1.0, 1.4 wt% for catalysts **3a**, **3b**, **3c**, **3d**, respectively (Table 1).

3.2 Catalytic activity

To evaluate the catalytic activities of FDU-supported gold(I) catalysts, the amination of *trans*-1,3-diphenyl-2-propen-1-ol with *p*-toluene sulphonamide was studied as a model reaction. Meeting atom economy demand, this reaction is an environment-friendly process since it generates water as the only by-product. The results summarized in Table 2 show the influence of the reaction parameters.

The homogeneous Ph_3PAuCl catalyst (0.5 mol%) afforded 67% product yield (Table 2, entry 1) in dioxane. In contrast, the immobilized catalyst **3a** afforded a 89% yield with 0.1 mol% Au loading (Table 2, entry 2). Other immobilized catalysts, **3b–d**, also showed excellent yield (Table 2, entries 3–5) though a much lower catalyst amount was used. In particular, sample **3d** could afford a 95% product yield in 1.5 h. The catalyst bearing electron-donating group – OMe in phosphine ligand required a longer reaction time to give a good product yield (Table 2, entries 3 and 4). When the catalyst amount was decreased to 0.05 mol%, all catalysts showed detrimental activity except for **3d** (Table 2, entries 6–9). The high activity of **3d** might be due to the strong electron-withdrawing effect of the $-CF_3$ group in the phosphine ligand.[39–42] Further, decreasing the amount of **3d** by tenfold to 0.01 mol% could still lead to a 50% yield after reaction for 8 h (Table 2, entry 10). Thus, **3d** was chosen for the subsequent study due to its high catalytic activity. The solvent-effect on the reaction was also studied (Table 2, entries 11–15). Among several commonly used solvents, the reaction proceeding in dioxane afforded the best yield. When homogeneous gold was supported on polystyrene[43] and SBA-15,[44,45] both catalysts showed lower activity than FDU-15 supported catalysts (Table 2, entries 16 and 17). No reaction was observed on using AgOTf as the catalyst. Interestingly, AgOTf could afford 29% product yield under dark condition (Table 2, entry 18), which is probably due to the light-sensitive nature of AgOTf.[46] This light-dependent activity was also observed for homogeneous

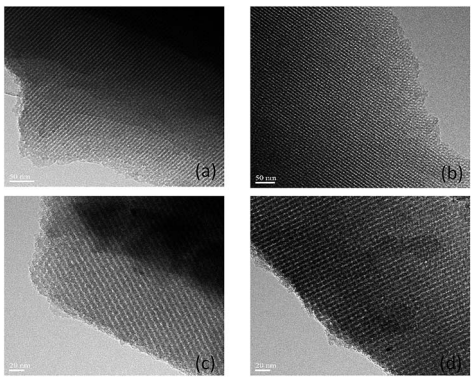

Fig. 3 TEM images of (a) FDU-15, (b) **1** (FDU-CH_2Cl), (c) **2d** and (d) **3d**.

Table 2 Screening of catalysts and reaction conditions for amination of allylic alcohols[a]

Entry	Catalyst	Au amount (mol%)	Solvent	Time (h)	Yield[b] (%)
1	Ph_3PAuCl	0.5	Dioxane	1.5	67 (85)[c]
2	**3a**	0.1	Dioxane	1.5	89
3	**3b**	0.1	Dioxane	4	90
4	**3c**	0.1	Dioxane	4	90
5	**3d**	0.1	Dioxane	1.5	95
6	**3a**	0.05	Dioxane	7	43
7	**3b**	0.05	Dioxane	20	38
8	**3c**	0.05	Dioxane	20	41
9	**3d**	0.05	Dioxane	1.5	91
10	**3d**	0.01	Dioxane	8	50
11	**3d**	0.05	MeCN	1.5	50
12	**3d**	0.05	$MeNO_2$	3	75
13	**3d**	0.05	THF	3	Trace
14	**3d**	0.05	DMF	3	n.r.
15	**3d**	0.05	DMSO	3	n.r.
16	SBA-PPh_2AuCl	0.5	Dioxane	1.5	73
17	PS-PPh_2AuCl	0.5	Dioxane	1.5	78
18	AgOTf	0.1	Dioxane	1.5	n.r (29)[c]
19	**2d**	0.1	Dioxane	24	n.r

[a] Reaction conditions: 1 mmol *trans*-1,3-diphenyl-2-propen-1-ol, 2 mmol *p*-toluene sulfonamide, 1 : 1 cat. (mol% Au)/AgOTf, 2 mL solvent, argon atmosphere. [b] Isolated yield. [c] Data in parentheses were yields avoiding light.

Ph_3PAuCl, which also provises better reactivity under dark conditions (Table 2, entry 2). This behavior effectively explains the enhanced activity of immobilized catalysts compared with the homogenous counterpart since the mesoporous wall may protect both AgOTf and Au-catalyst from light-driven decomposition. This detrimental effect could be prevented by the mesoporous wall of FDU-15, allowing for the formation of active species $Ph_3PAuOTf$.[47] It should be noted that no reaction was observed for sample **2d**, which did not contain any Au (Table 2, entry 19), further emphasizing the catalytic role of Au(I) centers.

Under the optimized reaction conditions, we then investigated the reactivity of different allylic alcohols and amine. The results are summarized in Table 3. Both the electron-withdrawing and electron-donating substituted aryl sulfonamides afforded the desired products in moderate to high yields (Table 3, entries 1–4). However, the use of electron-withdrawing groups required longer reaction times and higher temperatures. Aliphatic sulfonamide and benzyl carbamate also gave excellent yields (Table 3, entries 5 and 6). Even reactions starting with *p*-NO_2 and *p*-Cl substituted-aniline could proceed smoothly, affording the corresponding products with a high yield after a prolonged reaction time (Table 3, entries 7 and 8). Next, we investigated the scope of different allylic alcohols (**4b–4d**) using **5a** or **5b** as the coupling partner in most cases (entries 9–14). All these reactions proceeded at a lower rate than that of **4a** and resulted in moderate product yields at higher temperatures. The results show that **4b** afforded a 2 : 1 mixture of the α- and γ-substituted allylic sulfonamides at 51% overall yield (Table 3, entry 9). The reaction of **5b** also gave a mixture of the α- and γ-substituted products (Table 3, entry 10). The γ-products may be obtained *via* hydroamination reaction of the C–C double bond pathways.[48]

The recyclability of catalyst **3d** was also examined in the amination reaction of *trans*-1,3-diphenyl-2-propen-1-ol with *p*-toluenesulfonamide. The catalyst was recovered by simple filtration after reaction, washed with ethyl acetate and acetone and then dried in vacuum. The dried catalysts were directly used for the next catalytic cycle. As shown in Fig. 4, catalyst **3d** could be reused for at least twelve times without significant decrease in the isolated yield. We compared catalyst **3d** before and after 12 runs with different characterization in XPS, XRD and BET (Fig. S6–S8†). It can be clearly observed that the oxidation state of Au(I) was well retained for the spent catalyst (Fig. S6†).[49] The XRD pattern indicated that the ordered structure of organic frameworks collapsed to some extent after these runs (Fig. S7†). The BET result also indicated that the pore size and specific surface area decreased, in line with the collapse of the

Table 3 Reaction scope of different allylic alcohols and amine[a]

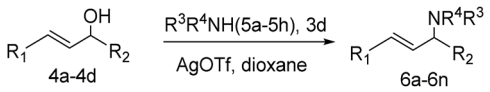

Entry	Allylic alcohols	Nucleophine	T (°C)	Time (h)	Product	Yield[b] (%)
1	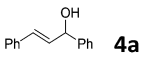 **4a**	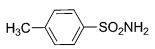 **5a**	30	1.5	**6a**	91
2	**4a**	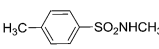 **5b**	30	4	**6b**	91
3	**4a**	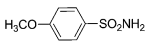 **5c**	30	1.5	**6c**	81
4[c]	**4a**	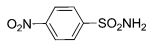 **5d**	50	26	**6d**	77
5	**4a**	$CH_3SO_2NH_2$ **5e**	50	7.5	**6e**	86
6[c]	**4a**	$CbzNH_2$ **5f**	30	2	**6f**	98
7[c]	**4a**	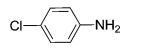 **5g**	50	26	**6g**	93
8	**4a**	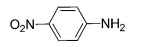 **5h**	30	12	**6h**	98
9	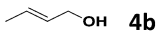 **4b**	**5a**	85	53	**6i**, **6i′**	51 (2 : 1)[d]
10	**4b**	**5b**	85	53	**6j**, **6j′**	48 (3 : 1)[d]
11	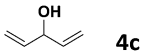 **4c**	**5a**	50	25	**6k**	48
12	**4c**	**5b**	50	25	**6l**	42
13	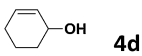 **4d**	**5a**	50	8	**6m**	56
14	**4d**	**5b**	50	9	**6n**	70

[a] Reaction conditions: 1 mmol allylic alcohols, 2 mmol nucleophile, **3d** (0.05 mol% Au), 0.05 mol% AgOTf, 2 mL dioxane, argon atmosphere. [b] Isolated yield. [c] 0.2 mol% **3d**, 0.2 mol% AgOTf. [d] The ratio of α-product to γ-product.

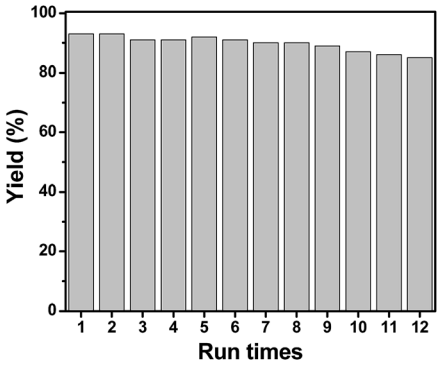

Fig. 4 The reusability of sample **3d** in the amination reaction of *trans*-1,3-diphenyl-2-propen-1-ol with *p*-toluenesulfonamide.

framework, which is probably responsible for the sharp decrease of product yield after twelve runs.

We further examined the utility of **3d** in the intramolecular cyclization for the synthesis of substituted 2,3-dihydro-4*H*-pyran-4-ones. The dihydropyranones moiety as one of the most important components has been observed in many naturally occurring products and displays a variety of biological activities.[50–60] After preliminary screening of the reaction conditions, catalyst **3d** could efficiently catalyze the intramolecular cyclization of **7a**, which provided results comparable to those obtained using homogeneous catalysts (Table 4, entry1). Benzene ring substituted 2,3-dihydro-4*H*-pyran-4-ones compounds **8a–k** were also synthesized in good yields using this heterogeneous catalyst(Table 4).

The reaction of substituted groups at the *para* position of the aryl ring proceeded efficiently (Table 4, entries 2, 5, 6, 9, 10 and 11). The reactions of substrates comprising strong electron-withdrawing groups such as $-CF_3$, $-NO_2$ and $-CN$ all gave the corresponding products in high yield (Table 4, entries 5, 9 and 10). The reactions were also carried out using the substrates with substituted groups on the other positions of the aryl ring (Table 4, entries 3, 4, 7 and 8). The aryl ring containing a chloro group at the *meta* position afforded a higher yield than those at the *para* and *meta* positions (Table 4, entries 6–8), while the methoxyl group led to a slightly lower yield (Table 4, entries 2–4). The catalyst can also be easily recycled.

Table 4 The intramolecular cyclization of **7a–7k**[a]

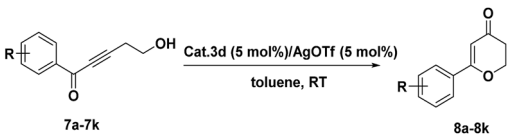

Entry	R	Product	Time (h)	Yield[b] (%)
1	H **7a**	**8a**	8	81
2	4-OCH_3 **7b**	**8b**	12	80
3	3-OCH_3 **7c**	**8c**	12	72
4	2-OCH_3 **7d**	**8d**	12	73
5	4-CF_3 **7e**	**8e**	48	84
6	4-Cl **7f**	**8f**	12	56
7	3-Cl **7g**	**8g**	24	80
8	2-Cl **7h**	**8h**	12	58
9	4-CN **7i**	**8i**	24	90
10	4-NO_2 **7j**	**8j**	24	83
11	4-Br **7k**	**8k**	12	78

[a] Reaction conditions: 0.45 mmol **7**; **3d** (5 mol% Au), and 5 mol% AgOTf; 4 mL toluene; argon atmosphere. [b] Isolated yield.

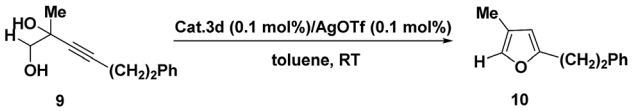

Scheme 2 The intramolecular cyclization of **9** to **10**.

Finally, we used **3d** as the catalyst for the synthesis of five-membered heterocyclic compounds. Furans are important intermediates, which widely serve as key structural subunits in numerous natural products, industrial organic syntheses and material science.[61–63] The reaction of propargyl alcohol **9** afforded the corresponding substituted furan **10** at 92% yield after 6 h, which shows similar activity to the homogeneous catalyst (Scheme 2).

4. Conclusions

In summary, we have developed a series of ordered mesopolymers FDU supported gold(I) catalysts (**3a–3d**). Catalyst **3d** showed the best catalytic activity in amination of allylic alcohols with different nucleophiles. Compared with homogeneous gold(I) catalyst, the heterogeneous gold(I) catalysts exhibited enhanced catalytic activity. The present study suggests the potential structural cooperation of the support material could enhance the stability. Moreover, the reaction also performed efficiently at a lower catalyst loading (0.05 mol%), which may be explained by the high dispersion of active sites in the mesopolymers and the catalysts can be easily recovered and recycled without significant decrease in activity. Catalyst **3d** was also applicable to other organic transformations, affording good yields. Further research for application of **3d** and other heterogeneous gold catalysts are now in progress.

Conflicts of interest

There are no conflicts to declare.

Acknowledgements

We acknowledge the financial support by NSFC (21373088, 21533002), China Ministry of Science and Technology (2016YFA0202804).

References

1 A. Hoffmann-Roder and N. Krause, *Org. Biomol. Chem.*, 2005, **3**, 387–391.
2 G. J. Hutchings, *Catal. Today*, 2005, **100**, 55–61.

3 A. S. K. Hashmi and G. J. Hutchings, *Angew. Chem., Int. Ed.*, 2006, **45**, 7896–7936.
4 A. Stephen and K. Hashmi, *Chem. Rev.*, 2007, **107**, 3180–3211.
5 Z. Li, C. Brouwer and C. He, *Chem. Rev.*, 2008, **108**, 3239–3265.
6 N. Marion and S. P. Nolan, *Chem. Soc. Rev.*, 2008, **37**, 1776–1782.
7 T. Yao, X. Zhang and R. C. Larock, *J. Am. Chem. Soc.*, 2004, **126**, 11164–11165.
8 Y. Liu, F. Song, Z. Song, M. Liu and B. Yan, *Org. Lett.*, 2005, **7**, 5409–5412.
9 M. H. Suhre, M. Reif and S. F. Kirsch, *Org. Lett.*, 2005, **7**, 3925–3927.
10 B. D. Sherry, L. Maus, B. N. Laforteza and F. D. Toste, *J. Am. Chem. Soc.*, 2006, **128**, 8132–8133.
11 G. Zhang, L. Cui, Y. Wang and L. Zhang, *J. Am. Chem. Soc.*, 2010, **132**, 1474–1475.
12 H. F. Jonsson, S. Evjen and A. Fiksdahl, *J. Am. Chem. Soc.*, 2017, **19**, 2202–2205.
13 M. J. Harper, E. J. Emmett, J. F. Bower and C. A. Russell, *J. Am. Chem. Soc.*, 2017, **13**, 12386–12389.
14 A. Corma, *Chem. Rev.*, 1997, **97**, 2373–2420.
15 C. M. Crudden, D. Allen, M. D. Mikoluk and J. Sun, *Chem. Commun.*, 2001, 1154–1155.
16 A. M. Liu, K. Hidajat and S. Kawi, *J. Mol. Catal. A: Chem.*, 2001, **168**, 303–306.
17 D. E. De Vos, M. Dams, B. F. Sels and P. A. Jacobs, *Chem. Rev.*, 2002, **102**, 3615–3640.
18 A. Taguchi and F. Schüth, *Microporous Mesoporous Mater.*, 2005, **77**, 1–45.
19 M. Guino and K. K. Hii, *Chem. Soc. Rev.*, 2007, **36**, 608–617.
20 R. A. Sheldon, *Chem. Soc. Rev.*, 2012, **41**, 1437–1451.
21 A. Corma, E. Gutiérrez-Puebla, M. Iglesias, A. Monge, S. Pérez-Ferreras and F. Sánchez, *Adv. Synth. Catal.*, 2006, **348**, 1899–1907.
22 W. Cao and B. Yu, *Adv. Synth. Catal.*, 2011, **353**, 1903–1907.
23 X.-Z. Shu, S. C. Nguyen, Y. He, F. Oba, Q. Zhang, C. Canlas, G. A. Somorjai, A. P. Alivisatos and F. D. Toste, *J. Am. Chem. Soc.*, 2015, **137**, 7083–7086.
24 W. Yang, L. Wei, F. Yi and M. Cai, *Catal. Sci. Technol.*, 2016, **6**, 4554–4564.
25 R. Cai, X. Ye, Q. Sun, Q. He, Y. He, S. Ma and X. Shi, *ACS Catal.*, 2017, **7**, 1087–1092.
26 J. T. Sarmiento, S. Suárez-Pantiga, A. Olmos, T. Varea and G. Asensio, *ACS Catal.*, 2017, **7**, 7146–7155.
27 M. Chen, Z.-M. Zhang, Z. Yu, H. Qiu, B. Ma, H.-H. Wu and J. Zhang, *ACS Catal.*, 2105, **5**, 7488–7492.
28 Y. Meng, D. Gu, F. Zhang, Y. Shi, H. Yang, Z. Li, C. Yu, B. Tu and D. Zhao, *Angew. Chem.*, 2005, **117**, 7215–7221.
29 F. Zhang, Y. Meng, D. Gu, Y. Yan, C. Yu, B. Tu and D. Zhao, *J. Am. Chem. Soc.*, 2005, **127**, 13508–13509.
30 R. Xing, N. Liu, Y. Liu, H. Wu, Y. Jiang, L. Chen, M. He and P. Wu, *Adv. Funct. Mater.*, 2007, **17**, 2455–2461.
31 R. Xing, Y. Liu, H. Wu, X. Li, M. He and P. Wu, *Chem. Commun.*, 2008, 6297–6299.
32 S. Yan, Y. Gao, R. Xing, Y. Shen, Y. Liu, P. Wu and H. Wu, *Tetrahedron*, 2008, **64**, 6294–6299.
33 R. Xing, H. Wu, X. Li, Z. Zhao, Y. Liu, L. Chen and P. Wu, *J. Mater. Chem.*, 2009, **19**, 4004–4011.
34 C. Yao, H. Li, H. Wu, Y. Liu and P. Wu, *Catal. Commun.*, 2009, **10**, 1099–1102.
35 W. Zhang, Q. Wang, H. Wu, P. Wu and M. He, *Green Chem.*, 2014, **16**, 4767–4774.
36 X. Giner, P. Trillo and C. Nájera, *J. Organomet. Chem.*, 2011, **696**, 357–361.
37 M. Egi, K. Azechi, M. Saneto, K. Shimizu and S. Akai, *J. Org. Chem.*, 2010, **75**, 2123–2126.
38 M. Egi, K. Azechi and S. Akai, *Org. Lett.*, 2009, **11**, 5002–5005.
39 J. P. Markham, S. T. Staben and F. D. Toste, *J. Am. Chem. Soc.*, 2005, **127**, 9708–9709.
40 P. Dubé and F. D. Toste, *J. Am. Chem. Soc.*, 2006, **128**, 12062–12063.
41 D. J. Gorin, B. D. Sherry and F. D. Toste, *Chem. Rev.*, 2008, **108**, 3351–3378.
42 W. Wang, G. B. Hammond and B. Xu, *J. Am. Chem. Soc.*, 2012, **134**, 5697–5705.
43 M. Egi, K. Azechi and S. Akai, *Adv. Synth. Catal.*, 2011, **353**, 287–290.
44 D. Zhao, Q. Huo, J. Feng, B. F. Chmelka and G. D. Stucky, *J. Am. Chem. Soc.*, 1998, **120**, 6024–6036.
45 X. Feng, M. Yan, T. Zhang, Y. Liu, M. Bao and X. Feng, *Green Chem.*, 2010, **12**, 1758–1766.
46 Q. Dong, N. Li, R. Qiu, J. Wang, C. Guo and X. Xu, *J. Organomet. Chem.*, 2015, **799–800**, 122–127.
47 J. Zhang, C.-G. Yang and C. He, *J. Am. Chem. Soc.*, 2006, **128**, 1798–1799.
48 P. Mukherjee and R. A. Widenhoefer, *Org. Lett.*, 2010, **12**, 1184–1187.
49 E. Aguiló, R. Gavara, J. Carlos Lima, J. Llorca and L. Rodríguez, *J. Mater. Chem. C*, 2013, **1**, 5538–5547.
50 M. M. Faul and B. E. Huff, *Chem. Rev.*, 2000, **100**, 2407–2474.
51 C. Yao, Z. Xiao, R. Liu, T. Li, W. Jiao and C. Yu, *Chem.–Eur. J.*, 2013, **19**, 456–459.
52 A. Ilangovan and P. Sakthivel, *RSC Adv.*, 2014, **4**, 55150–55161.
53 R. Aloise Pilli, L. Fernando Toneto Novaes, V. Maria Teixeira Carneiro, R. Lopes Drekener and C. Martins Avila, *Curr. Org. Chem.*, 2015, **12**, 523–529.
54 R. S. Coleman and E. B. Grant, *Tetrahedron Lett.*, 1990, **31**, 3677–3680.
55 J. D. Winkler and K. Oh, *Org. Lett.*, 2005, **7**, 2421–2423.
56 L. Candish and D. W. Lupton, *Chem. Sci.*, 2012, **3**, 380–383.
57 M. Reiter, S. Ropp and V. Gouverneur, *Org. Lett.*, 2004, **6**, 91–94.
58 M. Reiter, H. Turner, R. Mills-Webb and V. Gouverneur, *J. Org. Chem.*, 2005, **70**, 8478–8485.
59 X.-Z. Shu, X.-Y. Liu, K.-G. Ji, H.-Q. Xiao and Y.-M. Liang, *Chem.–Eur. J.*, 2008, **14**, 5282–5289.
60 F. Yang, K. G. Ji, S.-C. Zhao, S. Ali, Y. Y. Ye, X. Y. Liu and Y. M. Liang, *Chem.–Eur. J.*, 2012, **18**, 6470–6474.
61 L. Zhu, J. Luo and R. Hong, *Org. Lett.*, 2014, **16**, 2162–2165.
62 R. C. Brown, *Angew. Chem., Int. Ed.*, 2005, **44**, 850–852.
63 M. Zhang, H. F. Jiang, H. Neumann, M. Beller and P. H. Dixneuf, *Angew. Chem., Int. Ed.*, 2009, **48**, 1681–1684.